Electronic Supplementary Material (ESI) for Physical Chemistry Chemical Physics.

Supporting information for

In-Situ Observation of Potential-Dependent Structure of Electrolyte/Electrode Interface by Heterodyne-Detected Vibrational Sum Frequency Generation

Atsushi Sayama[1,2)], Satoshi Nihonyanagi*[1,3)], Yasuhiro Ohshima[2)] and Tahei Tahara*[1,2,3)]

1) *Molecular Spectroscopy Laboratory, RIKEN, Wako, Saitama 351-0198, Japan*
2) *Department of Chemistry, Tokyo Institute of Technology, Meguro, Tokyo 152-8551, Japan*
3) *Ultrafast Spectroscopy Research Team, RIKEN Center for Advanced Photonics (RAP), Wako, Saitama 351-0198, Japan*
*E-mail: nsatoshi@riken.jp, tahei@riken.jp

1. Estimation of the thickness of the solution layer

The thickness of the solution layer is estimated from the IR absorption of the CN stretch vibration of acetonitrile, which is observed in the un-normalized raw homodyne-detected VSFG spectrum of the acetonitrile/quartz interface, with the Lambert-Beer equation,

$$A = \varepsilon C l \quad , \tag{S1}$$

where, A, ε, C, l are the absorbance, molar extinction coefficient, concentration of chemical species and optical path length, respectively. The actual procedure of the estimation is as follows.

The absorption of acetonitrile was evaluated from the spectrum of the acetonitrile/quartz interface which was used as the reference spectrum. Figure S1 shows the un-normalized raw homodyne VSFG spectrum of the acetonitrile/quartz interface (red). The VSFG spectrum was fit to a Gaussian function (black), assuming a Gaussian spectral distribution of the input IR light. As clearly seen in this figure, a dip is recognized at 2250 cm^{-1}, which is due to the absorption of the CN stretch of acetonitrile in the solution layer. The transmittance was calculated to be 0.877 by dividing the observed signal intensity (red) with the fitted value (black) at 2250 cm^{-1}, and this evaluated transmittance was converted to absorbance,

$$A = -\log_{10} 0.877 = 0.0569 \quad . \tag{S2}$$

The molar extinction coefficient (ε) is calculated from the reported absorption cross section (σ~15×10^{-21} cm^2, [1]) of acetonitrile at 2250 cm^{-1} as,

$$\varepsilon = \log_{10} e \cdot \sigma \cdot N_A = 0.434 \times 15 \times 10^{-21} \times 6.022 \times 10^{23}$$
$$= 3.922 \times 10^3 \left[\frac{cm^2}{mol}\right] = 3.922 \times 10^{-1} \left[\frac{m^2}{mol}\right] \quad , \tag{S3}$$

where N_A is Avogadro constant. The molar concentration of acetonitrile is calculated as,

$$C = \frac{d\,[g\,m^{-3}]}{M\,[g\,mol^{-1}]} = 0.786 \left[\frac{g}{mL}\right] \times 10^6 \left[\frac{mL}{m^3}\right] \times \frac{1}{41.05} \left[\frac{mol}{g}\right]$$
$$= 19150 \left[\frac{mol}{m^3}\right] \quad . \tag{S4}$$

Here, d and M are the density and molecular weight, respectively, and the values were taken from the safety data sheet (SDS) provided by Sigma-Aldrich.

Then, the optical path length was calculated using the obtained A, ε and C as,

$$l = \frac{A}{\varepsilon C} = \frac{0.0569}{3.922 \times 10^{-1} \times 19150} = 7.58 \times 10^{-6}\,[m] \risingdotseq 7.6\,[\mu m] \quad . \tag{S5}$$

Consequently, the thickness of the solution layer was estimated to be ~8 μm, as described in the main text.

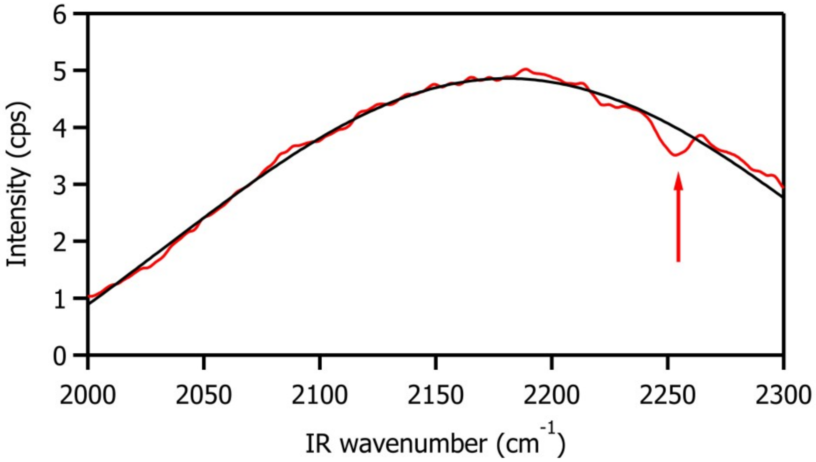

Fig. S1 Un-normalized raw homodyne-detected VSFG spectrum of the acetonitrile/quartz interface. The red curve shows the experimental data whereas the black curve is the fitting curve using a Gaussian function. A dip due to the absorption of acetonitrile in the solution layer is clearly recognized at 2250 cm^{-1} (marked by the red arrow).

2. Contribution of the $\chi^{(3)}$ effect

At the charged interfaces, molecules not only at the topmost layer but also in the diffuse electric double layer (EDL) can be oriented by the electric field and may contribute to the $\chi^{(2)}$ spectra. This contribution of the oriented molecules in the EDL is often called the $\chi^{(3)}$ effect. In order to show that the $\chi^{(3)}$ effect is negligible in the spectra shown in this paper, we estimate the thickness of diffuse EDL as follows.

The potential profile is obtained as a function of distance from the interface (x) by solving Poisson equation,[2] and the result is given by the following equation:

$$\phi = \frac{2k_BT}{ze}\ln\{\frac{1+gexp(-\kappa x)}{1-gexp(-\kappa x)}\},$$

$$g = \frac{\exp\left(\frac{ze\phi_0}{2k_BT}\right)-1}{\exp\left(\frac{ze\phi_0}{2k_BT}\right)+1},$$

$$\kappa = (\frac{2e^2N_Acz^2}{\varepsilon_r\varepsilon_0k_BT})^{1/2}, \qquad \text{(S6)}$$

where, ε_r, ε_0, k_B, T, e, c, z, and ϕ_0 are the relative dielectric constant, vacuum dielectric constant (= 8.854×10^{-12} C^2 J^{-1} m^{-1}), Boltzmann constant (=1.381×10^{-23} J K^{-1}), temperature (300 K), elementary charge (=1.602×10^{-19} C), concentration of electrolyte (in mol m^{-3}), valence of ion and potential applied to the electrode (potential at x=0), respectively. Using the relative dielectric constant of acetonitrile (38.8 [3]), κ is calculated as follows:

$$\kappa = (\frac{2\times(1.602\times10^{-19})^2\times6.022\times10^{23}\times0.1\times1000\times1^2}{38.8\times8.854\times10^{-12}\times1.381\times10^{-23}\times300})^{1/2}$$
$$= 1.474\times10^9\,[m^{-1}]\ . \qquad \text{(S7)}$$

The potential profile for ϕ_0 = 0.2 V, 0.6 V and 2.0 V are calculated and shown in Fig. S2. As seen in Fig. S2, the potentials drop precipitously at the very vicinity of the electrode (x<< 1 nm), in particular when a large potential is applied. This means that the strong electric field exists only at the very vicinity of the electrode and that the electric field in the diffuse EDL (Gouy-Chapman layer) is small in the present electrochemical condition. Thus, it is considered that the contribution of the molecules in the diffuse EDL in the $\chi^{(2)}$ spectra (the $\chi^{(3)}$ effect) is negligible, and the observed vibrational bands are attributable to the molecules at the very vicinity of the electrode interface.

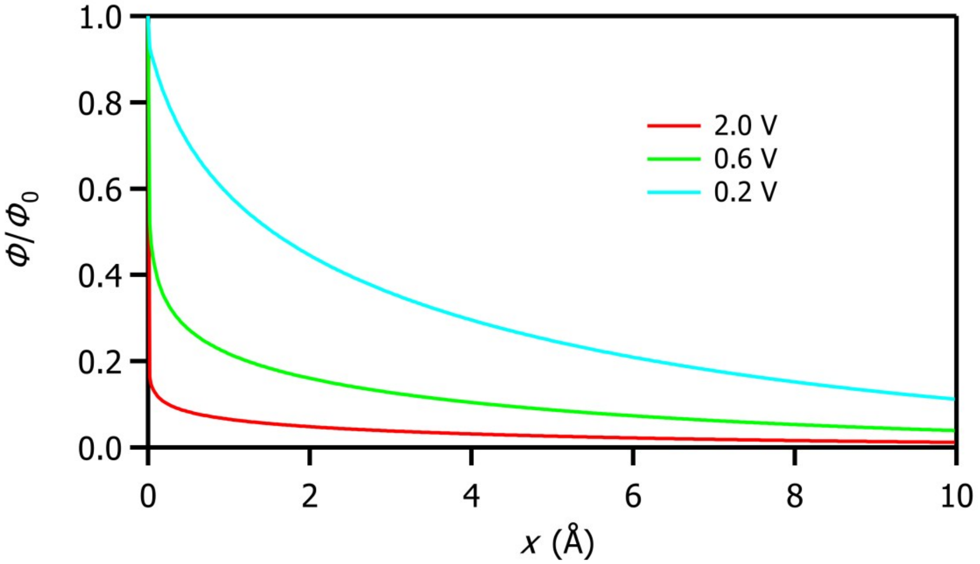

Fig. S2 Potential profile for the 0.1 M acetonitrile solution with various applied potentials.

3. Contribution of the CaF_2/acetonitrile solution interface

In principle, it is possible that the CaF_2 window/electrolyte solution interface in our spectro-electrochemical cell contributes to the SFG signal. However, because the electrode potential is applied only at the electrolyte/electrode interface, any signals that are dependent on the applied potential are safely attributable to the electrode interface. In the present study, all the observed vibrational bands vary depending on the potential and completely disappear at certain potentials. This potential dependence assures that these bands originate from the electrolyte/electrode interface, not from the CaF_2/electrolyte interface.

4. $\chi^{(2)}$ spectra of the air/acetonitrile interface

As we describe in Section 3-2 and 3-3 in the main text, we measured the $\chi^{(2)}$ spectra of the air/acetonitrile interface for experimentally discussing the relationship between the sign of the CH_3 and CN stretch bands and the up/down orientation of the acetonitrile. Figure S3a shows the $\chi^{(2)}$ spectra in the CH stretch region, where the CH_3 symmetric stretch band appears with the negative sign. This indicates the CH_3-up orientation at the interface, being consistent with the previous HD-VSFG study of monolayers having alkyl chains at the air/water interface.[4] On the other hand, in the Im$\chi^{(2)}$ spectrum in the CN stretch region (Fig. S3b) exhibits the CN stretch with the negative sign. These implies that the negative sign of the CN stretch indicates the CN-down orientation (and hence the CH_3-up orientation) of the acetonitrile molecule.

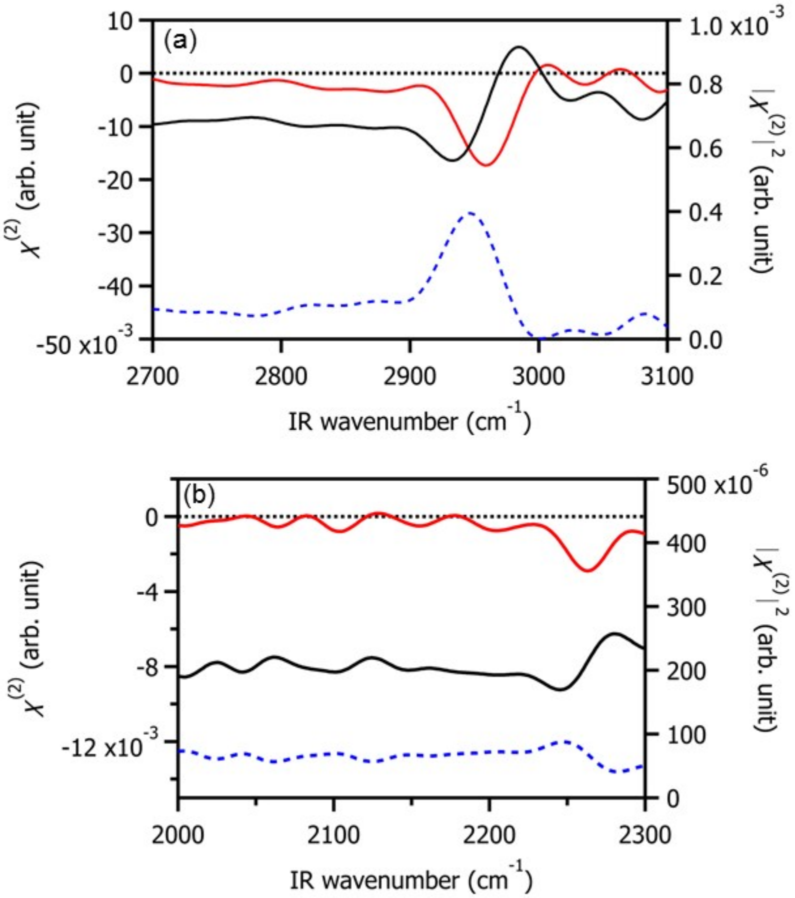

Fig. S3 $\chi^{(2)}$ and $|\chi^{(2)}|^2$ spectra of the air/acetonitrile interface in the (a) CH stretch and (b) CN stretch regions. The red and black solid curves represent Im$\chi^{(2)}$ and Re$\chi^{(2)}$ spectra, respectively. The blue broken curves represent $|\chi^{(2)}|^2$ spectra which were calculated from the Im$\chi^{(2)}$ and Re$\chi^{(2)}$ spectra. At this interface, the acetonitrile is expected to be in the CH_3-up (i. e., the CH_3 group points toward the air side)[5] and hence have the CN-down orientation.

5. Estimation of the IR loss due to the absorption by the $CF_3SO_3^-$ anion in the solution layer in the SO_3^- stretch region

Figure S4a shows the un-normalized raw homodyne-detected VSFG spectra of the electrolyte/quartz interface and the air/quartz interface. These spectra show two strong vibrational resonances at 1070 cm^{-1} and 1170 cm^{-1} due to the vibrational resonance of quartz itself, which prevents us to use quartz as the reference for the phase and amplitude calibration in this frequency region. The intensity ratio of these spectra is shown in Figure S4b. Although a peak-like feature is recognized at around 1150 cm^{-1}, this feature is an artifact originating from an incomplete normalization between the very small signals in the raw spectra in this frequency region. Except for this, the intensity ratio is almost featureless and, in particular, no spectral feature is recognized at 1040 cm^{-1} where the absorption due to SO_3^- stretch might appear. This indicates that the IR absorption by the $CF_3SO_3^-$ anion in the solution layer does not affect the VSFG spectra in this frequency region.

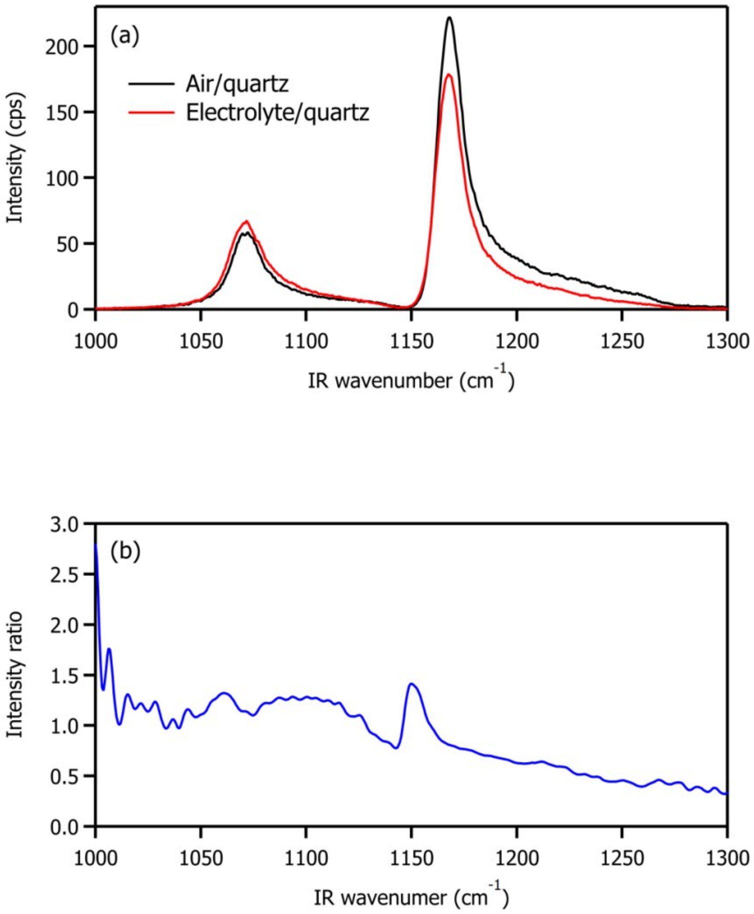

Fig. S4 (a) Un-normalized raw homodyne-detected VSFG spectra of the air/quartz and electrolyte/quartz interfaces. (b) Intensity ratio between the VSFG spectra of the electrolyte/quartz interface and the air/quartz interface.

6. Bulk IR and Raman spectra of 0.1 M $LiCF_3SO_3$ in acetonitrile solution

Figure S5a-c show IR and Raman spectra of 0.1 M $LiCF_3SO_3$ in acetonitrile. As described in Section 3-5 in the main text, the SO_3^- symmetric stretch band appears at 1040 cm^{-1} in the IR and Raman spectra with high and middle intensities, respectively, being consistent with the substantial intensity in the VSFG spectrum. On the other hand, although the CF_3 anti-symmetric band at 1160 cm^{-1} appears in the IR spectrum with a middle intensity, the corresponding band is hardly recognized in the Raman spectrum. It suggests very small intensity in the VSFG spectrum because the VSFG intensity is determined by the product of the IR and Raman intensities.

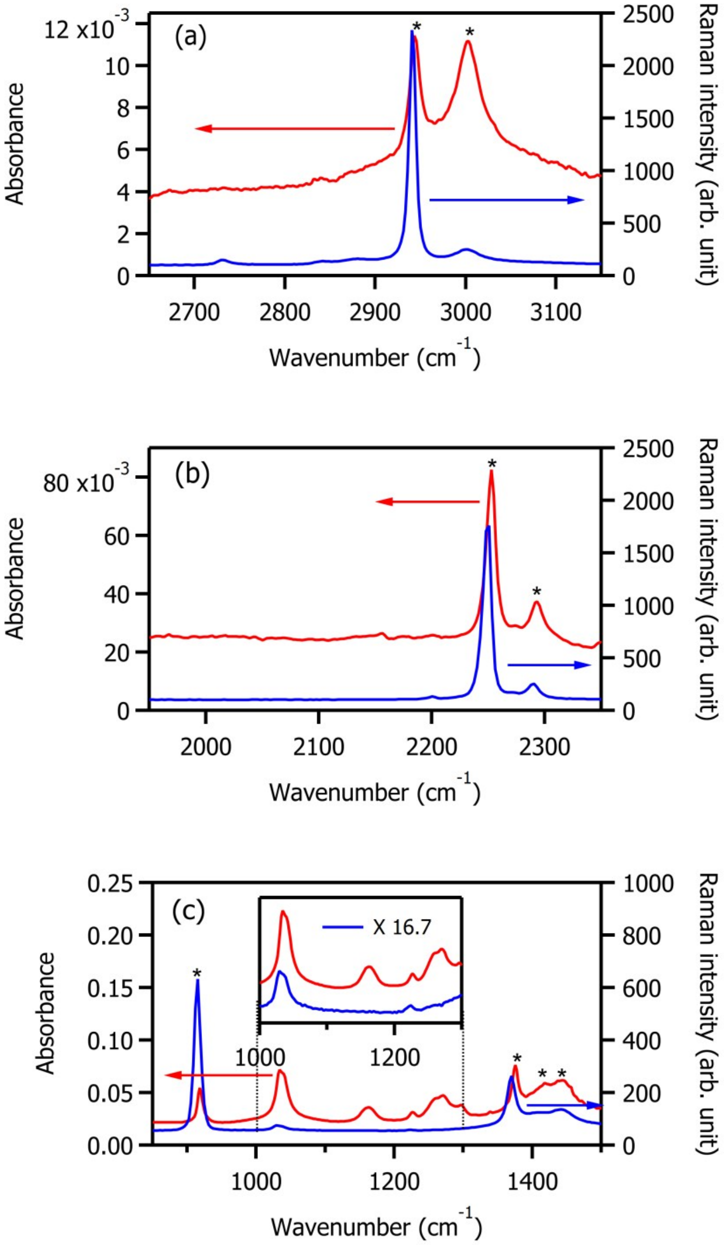

Fig. S5 Bulk IR (red) and Raman (blue) spectra of 0.1 M $LiCF_3SO_3$ in acetonitrile. (a) The CH_3 stretch region, (b) the CN stretch region, and (c) the anion band region. The assignments for the 2940-cm^{-1}, 2250-cm^{-1}, and 1040-cm^{-1} peaks are the CH_3 symmetric, CN, and SO_3^- symmetric stretch mode, respectively.[6-9] The peak around 3000 cm^{-1} in (a) is assigned to the CH_3 antisymmetric stretch, and the small peak at 2290 cm^{-1} in (b) is assigned to the combination band of the C-C stretch and CH_3 deformation which is enhanced by Fermi resonance.[6] The peak at 1160 cm^{-1} in the IR spectrum in (c) is attributed to the CF_3 anti-symmetric stretch. Note that the peaks marked by ★ are due to solvent acetonitrile.[6]

7. Fitting analysis

In Fig. 8 in the main text, we plot the electrode potential dependence of the amplitude of the CH_3 stretch and CN stretch bands of acetonitrile, CN^- band, and SO_3^- band. In order to quantitatively evaluate the amplitude of each band for making this plot, we performed the following fitting analysis on the $\mathrm{Im}\chi^{(2)}$ spectra obtained in the CH and CN stretch regions as well as the $|\chi^{(2)}|^2$ spectra in the frequency region of the SO_3^- band of the $CF_3SO_3^-$ anion.

An $\mathrm{Im}\chi^{(2)}$ spectrum contains vibrationally non-resonant and vibrationally resonant contributions and is given by the following formula, assuming Lorentzian bandshapes:

$$Im\chi^{(2)} = Im\chi^{(2)}_{NR} + \sum_q \frac{A_q\Gamma_q}{(\omega_q - \omega_{IR})^2 + {\Gamma_q}^2} \quad , \qquad \text{(S8)}$$

where $\chi^{(2)}_{\mathrm{NR}}$ is a vibrationally non-resonant background, A_q, ω_q, Γ_q are the amplitude, frequency and damping constant of q-th vibration mode, respectively. $\chi^{(2)}_{\mathrm{NR}}$ can take a complex value under the electronically resonance condition even if it is vibrationally non-resonant ($\chi^{(2)}_{\mathrm{NR}} = \mathrm{Re}\chi^{(2)}_{\mathrm{NR}} + i\mathrm{Im}\chi^{(2)}_{\mathrm{NR}}$). Eq. S8 is used for the fitting of $\mathrm{Im}\chi^{(2)}$ spectra in the CH stretch region in the main text, assuming a single vibrational resonance.

In case that inhomogeneous broadening of a resonant band is significant, a Gaussian distribution of the resonant mode needs to be considered. In the CN stretch region, a very broad negative band due to CN^- was observed, which is obviously broadened because of the inhomogeneity. For fitting this band, we simply replaced a Lorentz function with a Gaussian function, and the fitting function is represented in the following general form,

$$Im\chi^{(2)} = Im\chi^{(2)}_{NR} + \sum_q \frac{A_q\Gamma_q}{(\omega_q - \omega_{IR})^2 + {\Gamma_q}^2} + \sum_p B_p e^{-(\omega_p - \omega_{IR})^2/2\gamma_p^2} \quad . \qquad \text{(S9)}$$

Here, B_p and γ_p represent the amplitude and width of Gaussian function, respectively, which is used for fitting an inhomogeneously broadened p-th vibrational mode. Eq. S9 was used for the fitting of $\mathrm{Im}\chi^{(2)}$ spectra in the CN stretch region, using two Lorentzian functions (for two CN stretch bands of acetonitrile) and one negative Gaussian function (for the CN^- band).

The homodyne-detected VSFG spectra, which correspond to $|\chi^{(2)}|^2$ spectra, are represented by Eq. S10,

$$\begin{aligned} |\chi^{(2)}|^2 = {} & |\chi^{(2)}_{NR}|^2 + \sum_q \frac{{A_q}^2}{(\omega_q - \omega_{IR})^2 + {\Gamma_q}^2} \\ & + 2\sum_q \frac{Re\chi^{(2)}_{NR}A_q(\omega_q - \omega_{IR}) + Im\chi^{(2)}_{NR}A_q\Gamma_q}{(\omega_q - \omega_{IR})^2 + {\Gamma_q}^2} \end{aligned}$$

$$+\sum_{q\neq q'}\frac{A_qA_{q'}}{\left(\omega_q-\omega_{IR}-i\Gamma_q\right)\left(\omega_{q'}-\omega_{IR}+i\Gamma_{q'}\right)}\quad. \tag{S10}$$

Here, note that $\chi^{(2)}{}_{\mathrm{NR}}$ is a complex number, $\chi^{(2)}{}_{\mathrm{NR}} = \mathrm{Re}\chi^{(2)}{}_{\mathrm{NR}} + i\mathrm{Im}\chi^{(2)}{}_{\mathrm{NR}}$. Eq. S10 was used for the fitting of the SO_3^- stretch band measured with homodyne-detected VSFG.

References

1. C. P. Rinslanda, S. W. Sharpeb and R. L. Samsb, *J. Quant. Spectrosc. Radiat. Transf.*, 2005, **96**, 271-280.
2. A. J. Bard and L. R. Faulkner, *Electrochemical Methods: Fundamentals and Applications*, Wiley, New York, 2 edn., 2000.
3. *Rika Nenpyo (Chronological Scientific Tables 2014)*, Maruzen Publishing Co., Ltd., 2013.
4. S. Nihonyanagi, A. Sayama, Y. Ohshima and T. Tahara, *Chem. Lett.*, 2019, **48**, 1387-1390.
5. K. Saito, Q. Peng, L. Qiao, L. Wang, T. Joutsuka, T. Ishiyama, S. Ye and A. Morita, *Phys. Chem. Chem. Phys.*, 2017, **19**, 8941-8961.
6. P. Venlateswarlu, *J. Chem. Phys.*, 1951, **19**, 293-298.
7. D. H. Johnston and D. F. Shriver, *Inorg. Chem.*, 1993, **32**, 1045-1047.
8. J. M. Aliaay, Y. D. Meraa, H. G. M. Edwardsb, F. J. Garciaa and E. E. Lawsonb, *J. Mol. Struct.*, 1997, **408/409**, 439-450.
9. P. Geetha, M. Nair, C. Y. Panicker, H. T. Varghese, S. M. Y., K. Raju and P. S. A. Devi, *Orient. J. Chem.*, 2010, **26**, 167-170.